Supporting Information

Insights into the hybrid evaporation-spin coating method: process optimization and consequences for wide band gap perovskite solar cells

Zheng Zhang, [a,*] Ze Liu, [a,] Manlong Zhi, [a] Jiaqi Zhao, [a] Jie Lian, [a] Zhixing Yu,[a] Yingnan Guo,[a] Xiaoyang Liang,[a] Zhiqiang Li,[a,*]

Device Fabrication

ITO (150nm) coated glass substrates were cleaned and UV-Ozone treated following the procedures described above. To prepare the transporting layer, the substrates were transferred into an N_2-filled glovebox (O_2 and H_2O levels below 0.5 ppm). All the spin-coating conditions were optimised for the spin-coater integrated inside the glovebox. For the bottom hole transporting layer, we prepared PTAA solution with a concentration of 2 mg/ml in anhydrous Chlorobenzene. To spin the PTAA, we dropped the solution on the substrate and spin-coated it at 5000 rpm (1000 rpm/s) for 30 seconds. After the perovskite deposition, we annealed the film at 130ºC for different times to optimize the device performance. The best performance device was achieved with 30 mins annealing time. After the film cooled down to room temperature, PCBM(20 mg/ml) was spin-coated dynamically on the perovskite film at 2000 rpm for 30 seconds with the lid open. The buffer layer, Bathocuproine, was spin-coated dynamically on PCBM at 4000 rpm for 30

seconds. Finally, we evaporated 100 nm of Ag at 1 Å/s.

Perovskite Absorber Layer

The ITO/PTAA transferred into a vacuum chamber with a base pressure below 10^{-4} mbar for co-evaporating PbI_2 and CsBr. The sample was placed on a rotating plate,The PbI_2 and CsBr were placed in two separate crucibles and evaporated simultaneously to get a 250 nm lead iodides film.The optimized deposition rates for PbI_2 and CsBr were 6 Å/s and 0.6 Å/s). The evaporation rate was monitored by QCMs next to the substrate. The organic ammonium halide could be deposited both in nitrogen glove box. 80 μL 0.28 M solution of FAI:MABr:MACl (79:12:9) in isopropanol were spun onto the PbI_2 films at 2500 rpm for 30 s, then the film was annealed at 130 °C for 30 min in ambient air.

PEAI Passivation Process: Operational Steps

PEAI-L:All passivation processes were completed inside the glovebox. The sample was placed on the spin coater, and once the spin coater reached 5000 rpm, the PEAI solution was rapidly dropped onto the sample surface. The sample was then annealed at 100°C for 10 minutes.

PEAI-V:Drop the PEAI solution into the center of a Petri dish and swirl gently to ensure uniform distribution. Place the sample on a 100°C hotplate, then quickly invert the Petri dish and cover the sample. After 5 minutes, remove the Petri dish to complete the passivation process.

Experimental Section

Lead iodide (PbI_2, Purity>99.99%), Cesium chloride (CsBr, Purity>99.0%), Formamidine Hydroiodide(FAI, Purity≥99.5%),Methylamine bromide (MABr, Purity≥99.5%),Methylamine hydrochloride (MACl, Purity≥99.5%),Poly[bis (4-phenyl)(2,4,6-trimethylphenyl)amine (PTAA, Purity≥99.5%), Chlorobenzene (Purity≥99%) and propan-2-ol (IPA, Purity≥99.5%) were purchased from Sigma-Aldrich. [6,6]phenyl-C61-butyric acid methyl ester (PCBM, Purity≥99.5%), Bath ocuproine (BCP, Purity≥99.5%), phenylethyl ammonium iodide (PEAI, Purity≥99.5%)were purchased from Xi'an Polymer Light Co., Ltd.

Characterization and measurement:

The crystal structure was characterized by Bruker D8 Advance X-ray diffractometer (XRD) with Cu Kα radiation at 40 kV and 40 mA.The surface and cross sectional morphologies of the films were characterized by high resolution field emission scanning electron microscopy (SEM, FEI nova nano SEM 450). Atomic force microsco py (AFM) and scanning Kelvin probe force microscopy (KPFM) were performed using a Veeco Multimode 8 instrument. The optical properties of the thin film were characterized with a spectrophotometer (Perkin-Elmer Lambda 950). J-V measurements were performed under the standard test conditions (100 mW cm^{-2}, 25℃) using a 300 W xenon lamp (Model No. XES-100S1, SAN-EI, Japan). The EQE spectra were measured by a spectral response system (Enlitech QER3011) and calibrated by Si reference solar cells.

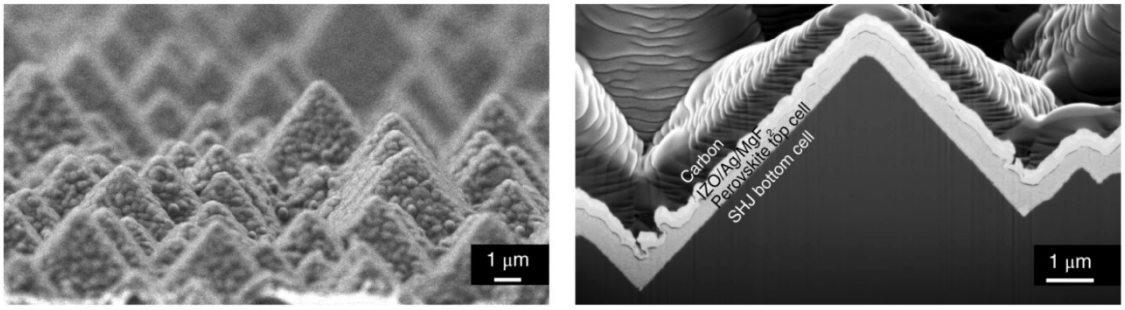

Figure S1 Secondary electron SEM image of the perovskite layer/textured Si through hybrid 2 step method (evaporation-spin coating). Copyright 2018, Nature Publishing Group.

Table S1 Input Process Parameters

Parameters	**Units**	**Low**	**High**
concentrat	Mg/ml	40	55
thickness	Nm	200	300
Substrate temperature	℃	25	100
Response	**Units**		
PCE	%		

Table S2 Parameters of the used CCD experimental design

Run	**Factor 1:** FAI concentration	**Factor 2:** Thickness	**Factor 3**: Substrate temperature

1	47.5	250	62.5
2	55	200	62.5
3	40	250	25
4	55	250	25
5	47.5	250	62.5
6	47.5	200	100
7	47.5	200	25
8	47.5	250	62.5
9	47.5	300	100
10	40	250	100
11	47.5	250	62.5
12	40	200	62.5
13	55	300	62.5
14	47.5	250	62.5
15	40	300	62.5
16	55	250	100
17	47.5	300	25

Table S3 ANOVA for selected factorial model of PCE

Source	Sum of Squares	Degree of freedom	Mean Square	F-value	P-value
Model	325.09	9	36.12	119.73	<0.0001
A-Thickness	0.48	1	0.48	1.58	0.2497
B-	103.68	1	103.68	343.65	<0.0001

Substrate temperature					
C-Concentration	3.19	1	3.19	10.57	0.0140
AB	0.016	1	0.016	0.052	0.8265
AC	19.71	1	19.71	65.34	<0.0001
BC	0.027	1	0.027	0.090	0.7726
A^2	28.36	1	28.36	94.02	<0.0001
B^2	110.29	1	110.29	365.56	<0.0001
C^2	40.74	1	40.74	135.03	<0.0001
Residual	2.11	7	0.30		
Lack of Fit	2.01	3	0.67	27.02	0.0041
Pure Error	0.099	4	0.025		
Cor Total	327.20	16			

Table S4 Equivalent circuit parameters of PSCs

	R_s (Ω)	R_{rec} (Ω)	C_μ (F)	τ_e (μs)
Control	11.63	810	$3.359*10^{-9}$	2.72
Target	9.181	2953	$3.18*10^{-9}$	9.39

Table S5 Porosity calculation of evaporated films

	Weight (mg)	Volume (mm^3)	Porosity (%)
	0.26	0.04225	0
Control (1)	0.232	0.03773	10.77
Control (2)	0.235	0.04064	9.62
Control (3)	0.240	0.03900	7.69
Control (ave)	0.2356	0.03912	9.38
Target (1)	0.206	0.033475	20.77
Target (2)	0.202	0.032825	22.41
Target (3)	0.209	0.033962	19.72
Target (ave)	0.2056	0.033421	20.93

Table S6. TRPL parameters of Control and Target passivated perovskite films

Parameter	T_{ave} (ns)	T_1 (ns)	T_2 (ns)	A_1	A_2
Control	89.6	45.6	120.4	0.59723	0.40182
Target	237.8	108.7	290.8	0.46438	0.42249

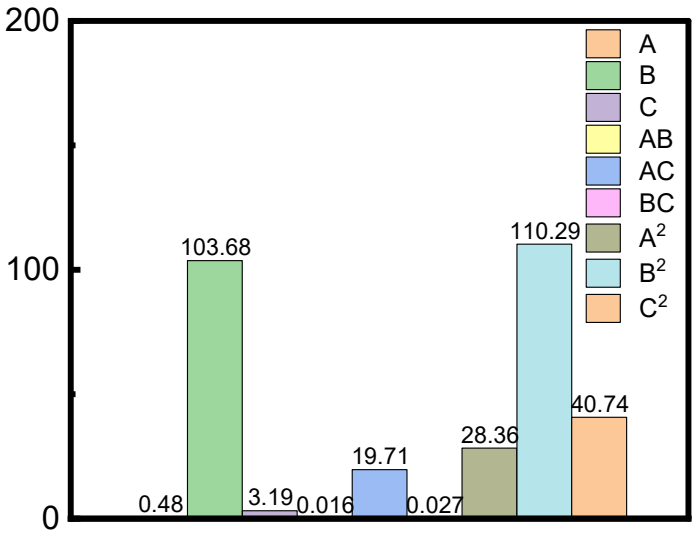

Figure S2 The effect degree of various factors on device PCE

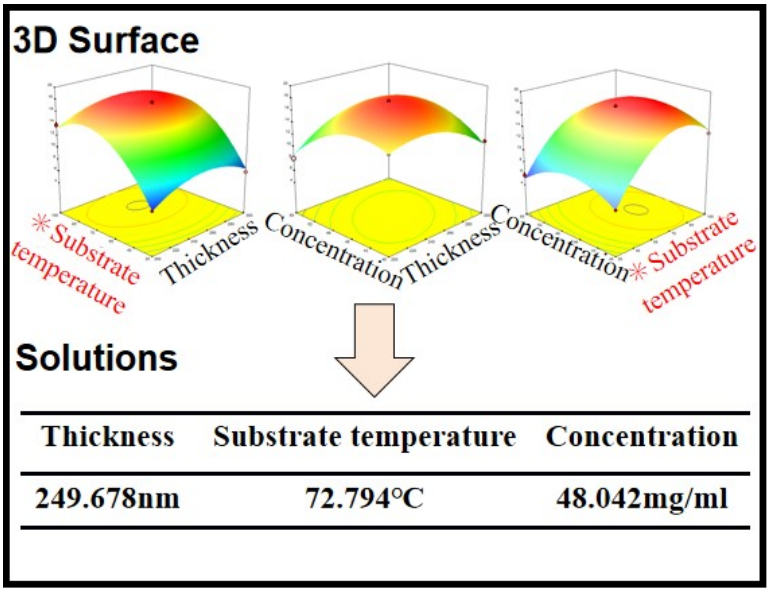

Figure S3 Optimal experimental condition confirmation logic

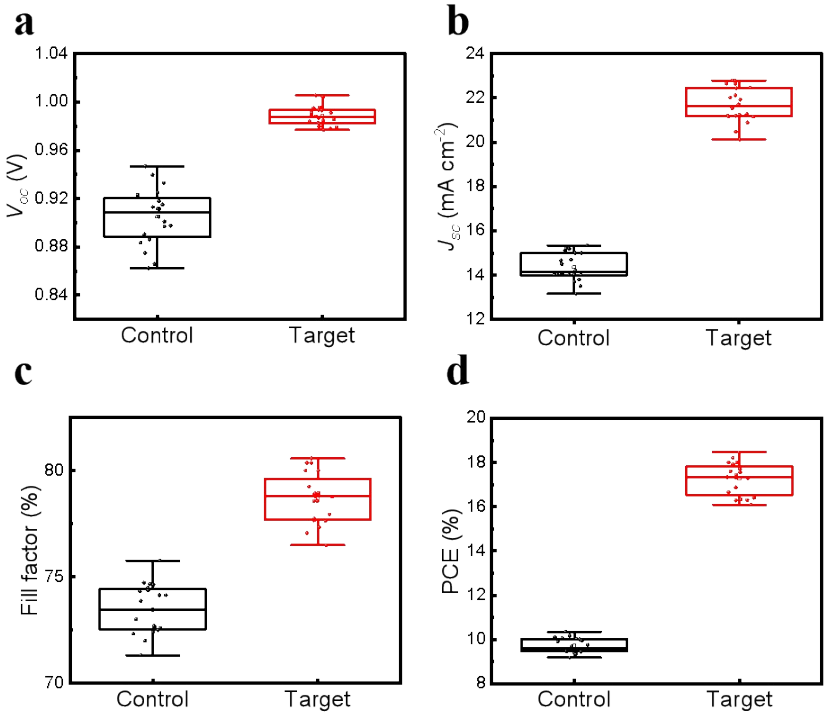

Figure S4 (a) Open-circuit voltage (V_{OC}), (b) short-circuit current density (J_{SC}), (c) fill factor (FF), and (d) power conversion efficiency (PCE) of the control and target solar cells.

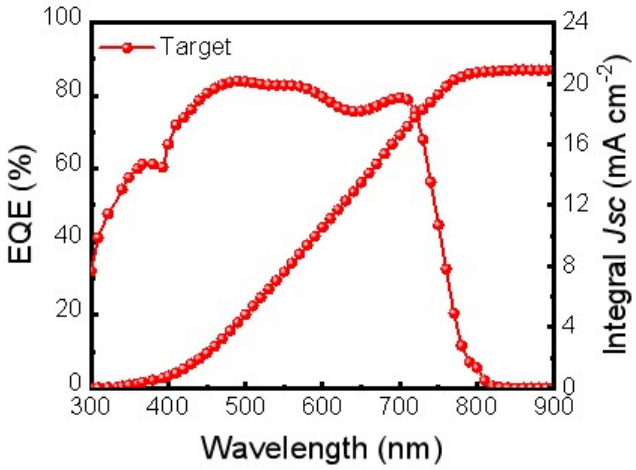

Figure S5 Incident photoelectric current conversion efficiency (IPCE) spectra and corresponding integrated current densities of the target devices.

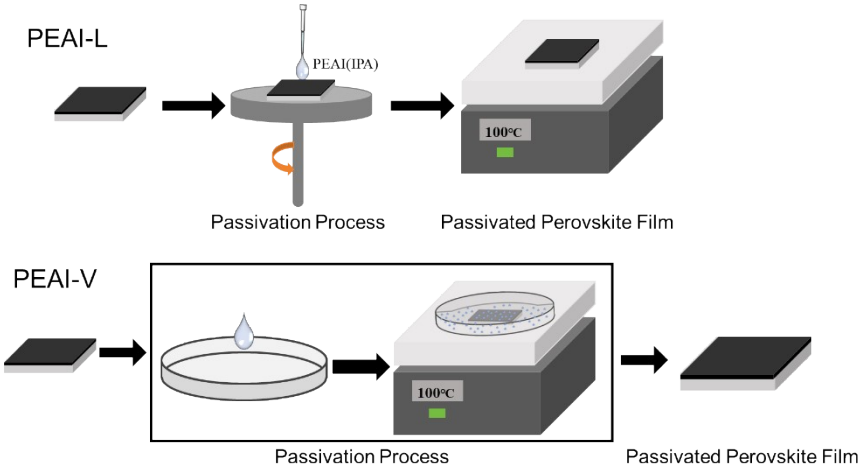

Figure S6 Schematic representation of the perovskite layer post treatment using PEAI liquid passivation (PEAI-L) and vapor passivation (PEAI-V)

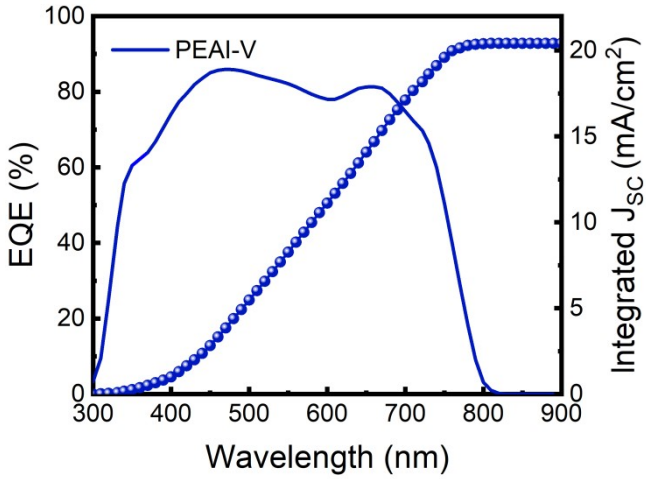

Figure S7 Incident photoelectric current conversion efficiency (IPCE) spectra and corresponding integrated current densities of the PEAI-V treated devices.

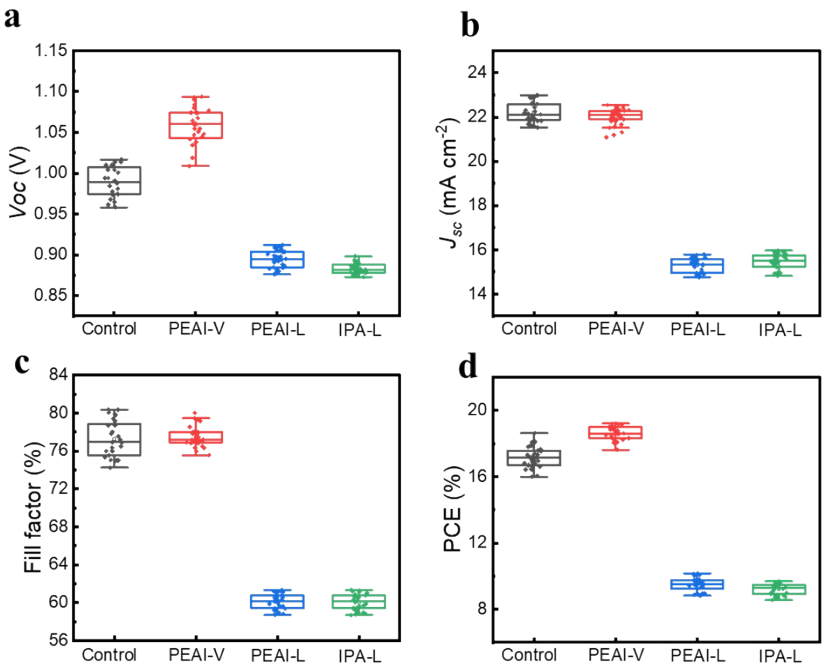

Figure S8 (a) Open-circuit voltage (V_{OC}), (b) short-circuit current density (J_{SC}), (c) fill factor (FF), and (d) power conversion efficiency (PCE) of the PEAI passivated devices

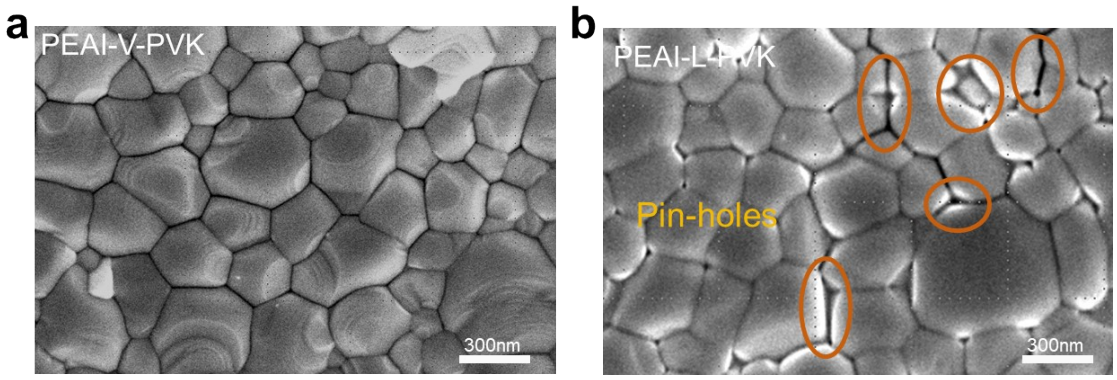

Figure S9 Top-viewed SEM images with PEAI vapor (a) and PEAI liquid (b) treatment

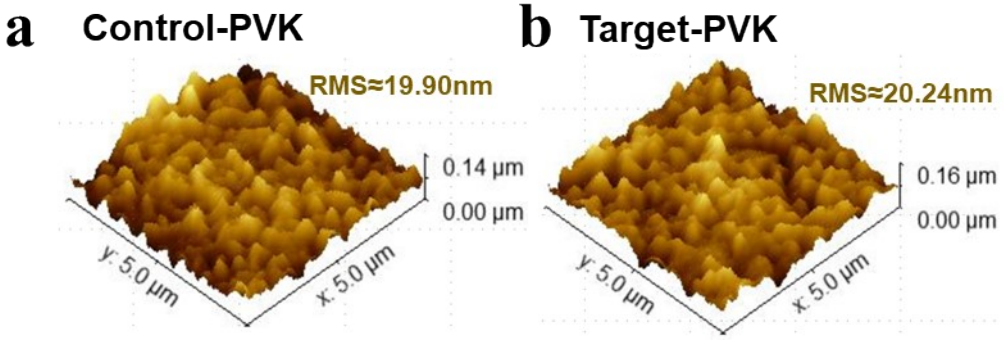

Figure S10 AFM images and corresponding RMS values of perovskite films (control-PVK; Target-PVK)

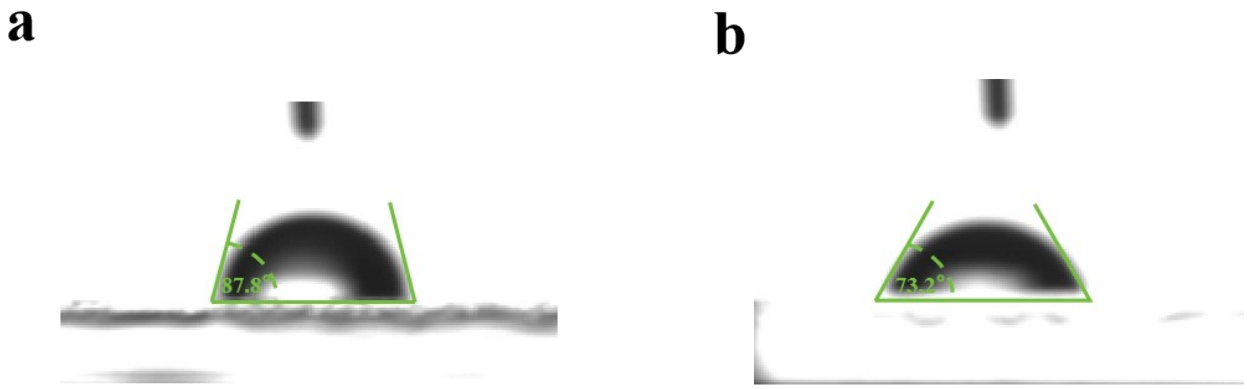

Figure S11 The water contact angle data of perovskite films (a) control and (b) target.

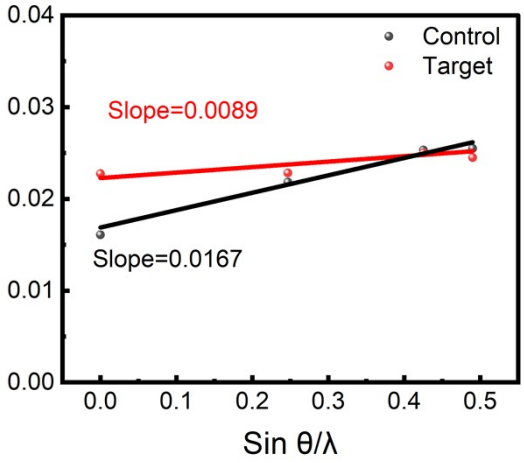

Figure S12 Williamson-Hall plot of perovskite films with control and target

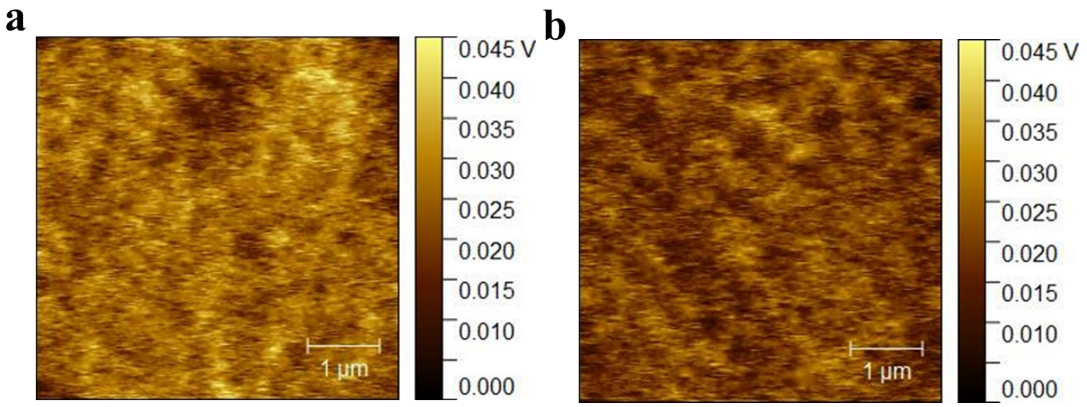

Figure S13 Surface potential images of perovskite films with control (a) and target (b) acquired by KPFM

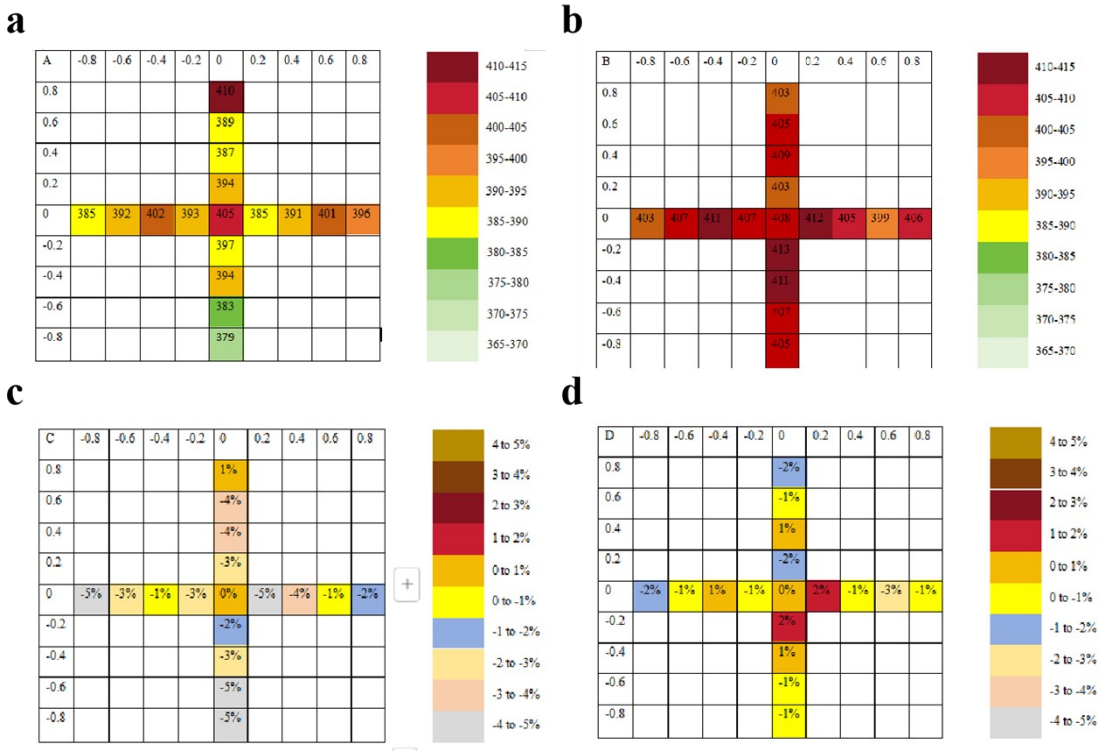

Figure S14 Perovskite thickness distributions at different points of the control (a) and target (b);(c,d)Perovskite thickness variation at different points (centimeters from the center "0") expressed as % difference from the thickness.

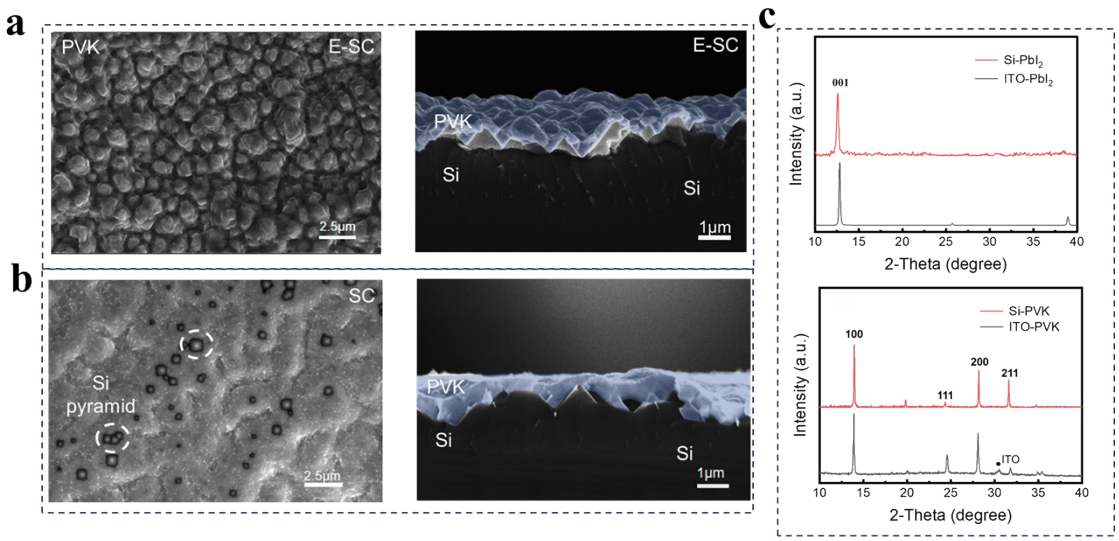

Figure S15 (a) Top-viewed, cross-sectional SEM and (b) XRD pattern images of perovskites fabricated on the textured silicon with hybrid evaporation/spin-coating route (E-SC); (c) Top-viewed and cross-sectional SEM of perovskites fabricated on the textured silicon with spin-coating route (SC)